

Electric Field Induced Magnetic Anisotropy in a Ferromagnet

S. J. Gamble,^{1,2} Mark H. Burkhardt,^{2,3} A. Kashuba,⁴ Rolf Allenspach,⁵ Stuart S. P. Parkin,⁶
H. C. Siegmann,¹ and J. Stöhr^{1,3}

¹*PULSE Center, Stanford University, Stanford, California 94025, USA*

²*Department of Applied Physics, Stanford University, Stanford, California 94305, USA*

³*Stanford Synchrotron Radiation Lightsource, Stanford, California 94305, USA*

⁴*Bogolyubov Institute for Theoretical Physics 14-b, Metrolohichna Street, Kiev 03680, Ukraine*

⁵*IBM Research, Zurich Research Laboratory, 8803 Rüschlikon, Switzerland*

⁶*IBM Almaden Research Center, San Jose, California 95120, USA*

(Received 8 December 2008; published 27 May 2009)

We report the first observation of a transient all electric field induced magnetic anisotropy in a thin film metallic ferromagnet. We generate the anisotropy with a strong ($\sim 10^9$ V/m) and short (70 fs) \vec{E} -field pulse. This field is large enough to distort the valence charge distribution in the metal, yet its duration is too brief to change the atomic positions. This pure electronic structure alteration of the sample generates a new type of transient anisotropy axis and strongly influences the magnetization dynamics. The successful creation of such an anisotropy opens the possibility for all \vec{E} -field induced magnetization reversal in thin metallic films—a greatly desired yet unachieved process.

DOI: 10.1103/PhysRevLett.102.217201

PACS numbers: 75.30.Gw, 75.40.Gb, 75.45.+j, 75.60.Jk

Magnetism is governed by three competing anisotropies determined by shape, internal strain, and crystallographic structure. Applications of magnetic materials correspondingly rely on controlling these anisotropies. Here we report the observation of a new type of transient magnetic anisotropy induced by applying a strong ultrashort electric field pulse. Since the nuclear positions remain unchanged on the 100-fs time scale ($1 \text{ fs} = 10^{-15} \text{ s}$) of our experiment, the effect arises solely through an \vec{E} -field induced distortion of the valence electron cloud. This distortion couples to the spin system via the spin-orbit interaction and generates the anisotropy in a way similar to how anisotropic bonding creates magnetocrystalline anisotropy.

The experiment utilizes the electric field of a highly relativistic electron bunch at the Final Focus Test Beam facility of the Stanford Linear Accelerator [1]. As a result of relativistic contraction, this field is entirely parallel to the surface of a sample oriented perpendicular to the direction of bunch propagation. Our sample is a thin film of magnetic metal and, since the field parallel to the sample surface must be continuous across the vacuum metal interface, the field penetrates into it. This generates the transient anisotropy which leads to a magnetization motion then detected in a switching pattern.

This stunningly simple, single shot experiment yields the first clear evidence of a new type of magnetic anisotropy generated by an \vec{E} -field induced distortion of valence states. It clearly demonstrates that a transient magnetic anisotropy can be created in a common magnetic metal by applying an \vec{E} field, and this makes important strides towards the ability of actively modifying magnetic properties by \vec{E} fields alone. This ability holds great interest for applications in spin electronics and magnetic recording. While effects of \vec{E} fields on magnetization have been seen

before [2–4], the desired “switching,” or reversal of the magnetization, has been elusive. Through the creation of the new transient anisotropy shown in this work, we provide the first clear path towards an all \vec{E} -field switching mechanism viable for normal ferromagnetic thin film metals at room temperature.

While a stationary electron has a spherically symmetric Coulomb field, an electron moving with relativistic speeds experiences a field compression so that the field is a flat, radially symmetric sheet perpendicular to the direction of motion [5,6]. Similarly, a bunch of relativistic electrons will have a field perpendicular to the beam direction. When such a normally incident bunch traverses a thin metal film, as illustrated in Fig. 1, the large \vec{E} field of the bunch is inserted into the metal film with the boundary condition $E_{\text{out}}^{\parallel} = E_{\text{in}}^{\parallel}$.

For a Gaussian bunch shape, the field amplitude has a longitudinal (z) Gaussian profile with standard (rms) deviation σ_z corresponding to a temporal rms pulse length of $\tau = \sigma_z/c$, where c is the speed of light. In the plane of the film the field depends on the rms perpendicular beam size σ_r according to [5,6]

$$\vec{E}(\vec{r}, t) = \frac{Q}{(2\pi)^{3/2} \epsilon_0 c r \tau} \left(1 - \exp\left[-\frac{r^2}{2\sigma_r^2}\right] \right) \exp\left[-\frac{t^2}{2\tau^2}\right] \frac{\vec{r}}{r}. \quad (1)$$

Here ϵ_0 is the vacuum dielectric constant, t the time, r the perpendicular distance from the bunch center, and Q the total electric charge. In our experiment the bunch had $Q = -2.6 \text{ nC}$ and was spherical with $\sigma_r = \sigma_z \approx 20 \text{ }\mu\text{m}$, corresponding to a rms pulse length of $\tau = 70 \text{ fs}$. The \vec{E} field is accompanied by a perpendicular magnetic field of strength $B = E/c$, as shown in Fig. 1.

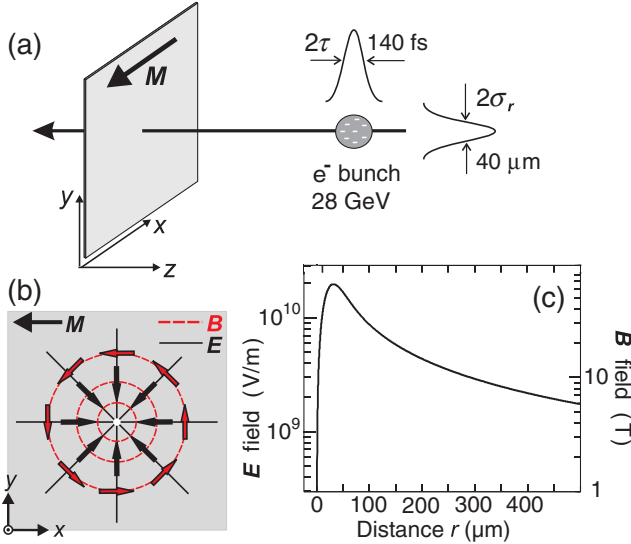


FIG. 1 (color online). (a) A Gaussian shaped electron bunch of 28 GeV and indicated standard (rms) deviations traverses a thin metallic ferromagnetic film perpendicular to the surface. The magnetization \vec{M} is initially set uniformly as shown. (b) The \vec{E} and \vec{B} fields are confined to a flat disk perpendicular to the beam and lie entirely in the x - y plane. (c) Plot of the maximum temporal E - and B -field amplitudes versus distance r from the beam center using the experimental longitudinal, $\tau = 70$ fs, and transverse, $\sigma_r = 20$ μm , rms beam sizes.

The metallic sample is a polycrystalline uniaxial 10 nm thick ferromagnetic film of $\text{Co}_{70}\text{Fe}_{30}$. It has a saturation magnetization at room temperature of $M = 2$ T, which corresponds to a shape anisotropy $K_s = 1.59$ MJ m^{-3} . The sample has a dominant in-plane uniaxial anisotropy energy density $K_u = 0.076$ MJ m^{-3} , obtained from magnetization curves along the hard axis and also by measuring the minimum \vec{B} field applied along the hard axis necessary to switch once. The film is capped with a 1.5 nm thick layer of Pt to prevent corrosion, and is sputter deposited onto a 0.5 mm thick $\text{MgO}(110)$ substrate with intervening buffer layers consisting mainly of 30 nm $\text{Cr}_{30}\text{Mg}_{20}$. The buffer layers both ensure a homogeneous deposition of the $\text{Co}_{70}\text{Fe}_{30}$ layer and provide the source of the uniaxial anisotropy.

Crucial to the experiment is that no screening of the bunch field can occur before its arrival at the sample surface because of the orientation of the field. Combining this with the fact that the 10 nm thickness of the film is smaller than the material's skin depth of 50 nm, the strong \vec{E} and \vec{B} fields are both present inside the sample.

Before exposure to the beam the sample is uniformly magnetized, and the electromagnetic field of the electron bunch then writes a characteristic domain pattern into it. The magnetic pattern generated by spin precession is retained by the sample as long as it stays below the Curie point $T_C \leq 1200$ K. We image the pattern long after the bunch has passed with spin sensitive scanning electron microscopy (spin-SEM or SEMPA). This technique is a

variant of a conventional SEM approach where the spin polarization of the emitted electrons is determined and, hence, a spatially resolved map of the magnetization direction is obtained. It is described in Ref. [7].

To interpret the pattern, it is necessary to separate effects generated by the \vec{B} field from those induced by the \vec{E} field. The torque due to $\vec{B} = \mu_0 \vec{H}$ is $\vec{T}_H = \vec{M} \times \vec{H}$ and since \vec{M} and \vec{H} are both in the sample plane, \vec{T}_H causes \vec{M} to move out of the plane of the film by an angle β . β depends on the sign and strength of \vec{T}_H , which varies in a characteristic way with the distance r from the beam center and the angle of \vec{M} with \vec{H} . Whether or not \vec{M} switches to the other direction depends on the angle β . The out-of-plane motion of \vec{M} creates a demagnetizing field, $H_D = -(1/\mu_0)M \sin\beta$, where μ_0 is the vacuum permeability, directed along the film normal. After the pulse, \vec{M} precesses about \vec{H}_D without external fields, and the size of H_D determines the precession angle and hence can induce switching by carrying \vec{M} across the hard in-plane axis. During precession the elevation angle β is reduced with time due to damping, and when it drops under some critical value determined by the static in-plane uniaxial anisotropy K_u of the film, the precession stops and regions of opposite magnetization may be formed.

The \vec{E} field does not act on \vec{M} directly but may modify the charge distribution. The charge anisotropy can then affect the magnetization through the spin-orbit coupling. While the conventional magnetocrystalline anisotropy arises from a charge anisotropy generated by the atomic positions and bonding, on ultrafast time scales a transient purely electronic distortion may exist of the valence charge within the atomic volume, without atomic motion. The expansion of such an \vec{E} -field induced anisotropy energy density \mathcal{E}_E must only contain even exponents to satisfy symmetry requirements and has the general form

$$\mathcal{E}_E = \varepsilon_0 + K_E = \varepsilon_0 - \varepsilon_2 \cos^2 \varphi - \dots \quad (2)$$

where ε_0 is isotropic and φ is the angle enclosed by \vec{E} and \vec{M} . K_E is the anisotropic spin-orbit energy density created by the \vec{E} -field distortion of the orbits. For our definition, $K_E \leq 0$ and $\varepsilon_2 \geq 0$. The sign of K_E here assumes \mathcal{E}_E is at a minimum when \vec{M} is aligned parallel with \vec{E} . Symmetry tells us, however, that the perpendicular orientation could also be the preferred one. If this is the case, fitting our experimental data to Eq. (2) will simply produce reversed signs for the constants. The creation of a new \vec{E} -field induced anisotropy axis generates a torque on \vec{M} of magnitude $|T_E| = |\partial \mathcal{E}_E / \partial \varphi| = |2\varepsilon_2 \sin \varphi \cos \varphi|$. It acts on \vec{M} as long as the \vec{E} field is present; hence its transient nature.

Like \vec{T}_H , \vec{T}_E causes \vec{M} to move out of the plane of the film by an angle which varies with the distance r from the beam center and the angle of \vec{E} with \vec{M} . We cannot quantify this dependence *a priori*, however, and must derive it from the recorded data. Since we know what pattern a \vec{B} field

alone produces, we can observe any variations from the expected pattern to elucidate the effect of the transient anisotropy introduced by \vec{E} .

Figure 2 shows the SEMPA image of the beam induced magnetic domains. Regions are seen as black and white contrast representing the switched and unswitched regions, respectively. The sequence of black and white circles counts the precession angle. The precession frequency ω acts as an internal clock measuring the time after the pulse at which the switch occurred, similar to the year rings in the trunk of a tree. We have $\omega = \Gamma H_D$, where $\Gamma = (g/2) \times (e/m_e)\mu_0$ is the gyromagnetic ratio which depends on the material specific g factor, the charge-to-mass ratio (e/m_e) of the electron, and μ_0 . The domains close to the point of impact between the two ring systems are asymmetric and might be generated by magnetic aftereffects [8]. Also present is a small left-right asymmetry which can be attributed to a bunch with a slightly elliptical cross section. Finally, a blurring of the boundary between switched and unswitched regions is observed due to the formation of zigzag domain walls, as noted in [9,10]. Most importantly, however, the pattern exhibits a marked up-down asymmetry, which was also observed on samples of different composition and magnitude of the uniaxial magnetic anisotropy. It strongly deviates from the more circular patterns observed in previous measurements with much longer field pulses having standard deviations of 2.1 and 4.4 ps ($1 \text{ ps} = 10^{-12} \text{ s}$) and about 50-fold weaker field amplitudes [9,10]. It is also distinct from the slight deformation observed in previous patterns due to the start of the precession of \vec{M} in the anisotropy fields of the sample, while the longer and weaker field pulses were still present [11]. In the present case, the stronger and shorter beam fields completely dominate, and the observed flattening of the pattern is a new characteristic effect.

In Fig. 3 three patterns are calculated with the Landau-Lifshitz-Gilbert (LLG) equation [6]. Simulation (a) is calculated with the regular LLG equation including the \vec{B} field only and a damping constant $\alpha = 0.015$, as in [10,11]. It

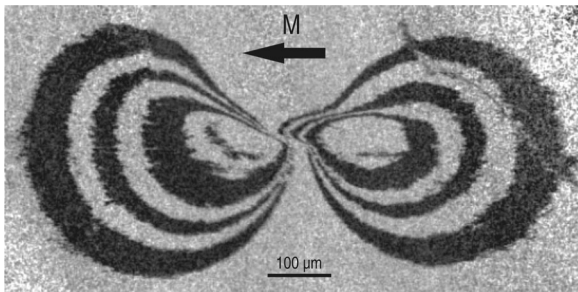


FIG. 2. Experimental magnetic pattern generated by a single $\tau = 70 \text{ fs}$ electron bunch in the experimental geometry of Fig. 1 for an in-plane uniaxial 10 nm thick ferromagnetic film of $\text{Co}_{70}\text{Fe}_{30}$ on $\text{MgO}(110)$. The pattern was determined by SEMPA [7]. In the light gray regions, \vec{M} points into the preset direction as shown while in the dark regions \vec{M} has switched into the opposite direction.

also includes the aforementioned precession in the sample's anisotropy fields during the pulse [11]. The simulation can account solely for the width of the outermost two black rings, not for the shape or number of rings. Two additional terms are needed to reproduce the experiment. One of these terms is due to the fact that the LLG equation in its original form does not account for spin-wave instabilities occurring in the large angle precession of \vec{M} about the demagnetizing field after the field pulse [9,12,13]. In Ref. [13] the equation of motion for magnetization precession shows that the precession is always unstable and is accompanied by a growing spin-wave instability. The feedback effect of spin waves on the precession of the uniform mode can be described in terms of a Gilbert damping constant which depends on the state of the spin-wave modes which grow exponentially with time. Therefore, we model the spin-wave instability by a local Gilbert constant $\alpha_{\text{in}}(t, \vec{r})$ that grows exponentially with time t according to $d\alpha_{\text{in}}/dt = \gamma |M^z(t, \vec{r})/M_0| \alpha_{\text{in}}(t, \vec{r})$. Here γ is the dimensionless increment of the instability. The instability growth rate is proportional to the local precession frequency in the field $H_D \sim M^z(t, \vec{r})$ about the sample normal; hence, no precession means no instability growth. The integration constant is determined according to

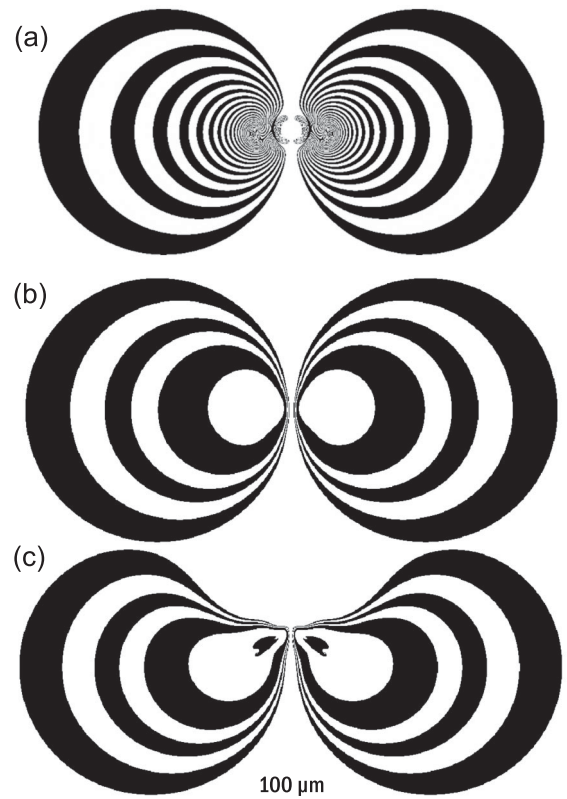


FIG. 3. Magnetic patterns calculated with the LLG equation. (a) Assuming that only a \vec{B} field is inside the sample and that the damping of the precession is constant in time, (b) \vec{B} field only but damping increases exponentially with time, (c) \vec{B} and \vec{E} field are present and the damping increases according to the text. Pattern (c) reproduces the main features of the experiment Fig. 2.

Fermi's golden rule for the probability to excite a spin wave in second order perturbation. The total dissipation constant is the sum of the intrinsic and the instability terms: $\alpha(t) = \alpha_0 + \alpha_{\text{in}}(t)$. The parameters used in the simulation of patterns (b) and (c) in Fig. 3 are $g = 2$, $K_u/K_s = 0.041$, $\gamma = 1.46$, and the intrinsic Gilbert dissipation constant $\alpha_0 = 0.017$. The spin-wave instabilities develop on a time scale ≥ 100 ps, that is long after the bunch has passed. Their inclusion accounts for the observed number of rings and their variable widths.

However, the deviation of the pattern from the circular shape can only be obtained if one also considers the effect of the \vec{E} field according to Eq. (2). A simulation including \vec{T}_E and assuming the parallel configuration between \vec{E} and \vec{M} is favored is shown in Fig. 3(c). It shows \vec{T}_E is opposed to the torque \vec{T}_H in the upper part of the pattern and adds to it in the lower part, which matches the observations. This shows the induced anisotropy axis is indeed parallel to \vec{E} . The deviation of the experimental pattern in Fig. 2 from the circular shape is thus direct evidence for the existence of a transient anisotropy inside the metallic sample during the field pulse. The anisotropy field induced by \vec{E} must be gigantic as it has to rival the magnetic beam field of tens of tesla.

To quantify the transient anisotropy energy density K_E in Eq. (2) from the experimental pattern we investigated various approximations. We obtain the best fit of the data by representing the transient anisotropy as a series expansion of the Legendre spherical harmonics about the direction of the \vec{E} field. We retain only $L = 2$ and $L = 4$ harmonics in our model:

$$K_E = -\varepsilon_2(E)\cos^2\varphi - \varepsilon_4(E)\cos^4\varphi. \quad (3)$$

We approximate the two transient anisotropies (the easy-axis and the fourth-order) by two rational functions: $\varepsilon_2(E) = \mathcal{E}_0[(b_2\mathcal{E}^2 + c_2\mathcal{E}^4)/(1 + \mathcal{E}^4)]$ and $\varepsilon_4(E) = \mathcal{E}_0[b_4\mathcal{E}^4/(1 + \mathcal{E}^4)]$. Here b_2 , c_2 , b_4 are adjustable parameters of the model, and the anisotropy energy density $\mathcal{E}_0 = ME_0/\mu_0c$ and normalized field $\mathcal{E} = E/E_0$ account for the fact that $\varepsilon_2(E)$ and $\varepsilon_4(E)$ saturate near the bunch. In our best fit, $b_2 = 0.74$, $c_2 = 0.78$, $b_4 = 0.41$, and $E_0 = E(r = 120 \mu\text{m})$. This corresponds to a time-averaged saturation anisotropy around 40 MJ m^{-3} , which, to our knowledge, is the largest magnetic anisotropy observed so far in a magnetic metal. It is significantly larger than the static magnetic anisotropy energy density of 17 MJ m^{-3} of hexagonal SmCo_5 [14] and larger anisotropies have so far been observed only for isolated Co atoms and clusters on a Pt(111) surface [15].

While this experiment uses a combination of applied \vec{B} and \vec{E} fields to determine the final state of magnetization, it suggests the possibility of switching the magnetization in a thin film by applying an \vec{E} field alone. The only criterion for switching is the induction of a sufficient in-plane anisotropy density K_E , so that the associated torque rotates

\vec{M} out of plane by a sufficient angle during the pulse, such that it can later precess around H_D across the hard in-plane axis. Since the anisotropy energy is an even function of E , mostly $\propto E^2$, it should be possible to use a linearly polarized photon pulse instead of the dc pulse used by us. This has the advantage that the linear B -field effects will cancel over a full wave cycle, opening the possibility for all electric field control of the magnetization of a normal metal at room temperature. This result is of particular interest when compared to those obtained in ultrafast demagnetization experiments. Beginning with the pioneering work of Beaurepaire *et al.* [16], experiments have consistently shown a rapid decrease in magneto-optic signals from magnetic materials following excitation with femtosecond optical pulses. While we do not probe our system on the femtosecond time scale, we do observe a final state produced by dynamics which occurred during our single fast electron pulse. This means our ultrafast nonoptical wavelength excitation technique does not randomize the magnetization, and rather controls it on the femtosecond time scale.

SLAC is supported by the U.S. DOE Office of Science, and the experimental program of the SLAC authors by the Office of Basic Energy Sciences. We wish to thank I. Tudosa for his help and advice during the exposure of the films, R. Iverson for focusing the electron beam, Clive Field for measuring the beam focus, and G.J. Collet for help with the sample chamber.

-
- [1] P. Emma *et al.*, in *Proceedings of the IEEE Particle Accelerator Conference, Chicago, 2001* (IEEE, Piscataway, NJ, 2001), pp. 4038–4040.
 - [2] M. Weisheit *et al.*, *Science* **315**, 349 (2007).
 - [3] Y.-H. Chu *et al.*, *Nature Mater.* **478**, 7 (2008).
 - [4] D. Chiba *et al.*, *Nature (London)* **455**, 515 (2008).
 - [5] J.D. Jackson, *Classical Electrodynamics* (Wiley, New York, 1999).
 - [6] J. Stöhr and H.C. Siegmann, *Magnetism: From Fundamentals to Nanoscale Dynamics*, Springer Series in Solid-State Sciences Vol. 152 (Springer, New York, 2006).
 - [7] R. Allenspach, *IBM J. Res. Dev.* **44**, 553 (2000).
 - [8] S. Chikazumi and C.D. Graham, *Physics of Ferromagnetism* (Oxford University, New York, 1997).
 - [9] C. Stamm *et al.*, *Phys. Rev. Lett.* **94**, 197603 (2005).
 - [10] C.H. Back *et al.*, *Science* **285**, 864 (1999).
 - [11] Ioan Tudosa, Ph.D. dissertation, Stanford University, 2005.
 - [12] A. Yu. Dobin and R.H. Victora, *Phys. Rev. Lett.* **90**, 167203 (2003).
 - [13] A. Kashuba, *Phys. Rev. Lett.* **96**, 047601 (2006).
 - [14] R. Skomski, *J. Phys. Condens. Matter* **15**, R841 (2003).
 - [15] P. Gambardella *et al.*, *Science* **300**, 1130 (2003).
 - [16] E. Beaurepaire, J.-C. Merle, A. Daunois, and J.-Y. Bigot, *Phys. Rev. Lett.* **76**, 4250 (1996).